Available online at www.sciencedirect.com
ScienceDirect
Geochimica et Cosmochimica Acta 71 (2007) 2072–2078
Geochimica et Cosmochimica Acta
www.elsevier.com/locate/gca

Synthesis of nitrate sodalite: An *in situ* scanning calorimetric study

Qingyuan Liu, Alexandra Navrotsky *

Thermochemistry Facility and NEAT ORU, University of California at Davis, Davis, CA 95616, USA

Received 8 September 2006; accepted in revised form 11 January 2007; available online 18 January 2007

Abstract

The formation of nitrate sodalite, an important constituent of the resilient heels at DOE nuclear waste storage sites, was closely followed by oven synthesis, *in situ* calorimetry as a function of heating rate from 0.01 to 0.1 °C/min and X-ray diffraction. A transition sequence of amorphous–zeolite A–sodalite–cancrinite was confirmed. For *in situ* synthesis calorimetry, the heat flow peaks related to zeolite A formation are shifted to higher temperatures as heating rate increases. Although the end products are mostly nitrate sodalite, no calorimetric signals associated with zeolite A to sodalite conversion are detected. This suggests that the enthalpy of formation of zeolite A and sodalite are very similar and the zeolite A to sodalite conversion enthalpy is small. This conclusion is in accord with previous measurements by oxide melt solution calorimetry.

1. INTRODUCTION

The leakage of high-level nuclear waste from the storage tanks at US Department of Energy (DOE) sites contaminates groundwater and interacts with surrounding sediments to form zeolite A, cancrinite and sodalite (Bickmore et al., 2001; Wan et al., 2002; Qafoku et al., 2003, 2004). The nature of contaminant transport in the vadose zone, a region of variable water content at the Hanford site, is not yet fully understood (Wan et al., 2002). The high volume precipitation of both amorphous and crystalline aluminosilicates from highly alkaline waste streams also interferes with several waste processing procedures. Due to plugged waste transfer lines, an evaporator for tank waste volume-reduction was shut down (Mattigod et al., 2002). The performance of a crystalline silicotitanate (CST) ion exchanger was degraded when such deposits were built up on its surface (Su et al., 2000). To better understand the occurrence and removal of aluminosilicates at DOE storage sites, the thermodynamic properties of such materials have been investigated in our laboratory (Liu et al., 2005; Moloy et al., 2006; Liu et al., 2007). However, the kinetics of formation and transformation of these phases is an equally important issue.

In situ calorimetry is a powerful tool for investigation of thermal events related to zeolite synthesis, such as enthalpy of mixing in solution (Yang and Navrotsky, 2004a), crystallization driving forces (Yang and Navrotsky, 2000, 2004b), and crystallization kinetics (Yang and Navrotsky, 2002). The major advantage of this method is the direct and continuous monitoring of reaction progress with heating in a closed system which does not lose water. When coupled with structural analysis (XRD, IR, NMR and microscopy) and solution characterization (species concentration and pH), the calorimetric signals can be intimately associated with subtle changes in solution speciation, solution reaction and structural evolution of the precipitate. We report findings on the synthesis of nitrate sodalite, combining oven synthesis, *in situ* synthesis calorimetry and X-ray diffraction analysis.

2. SAMPLE SYNTHESIS AND CHARACTERIZATION

ACS grade sodium silicate ($Na_2SiO_3{\cdot}9H_2O$, Fisher), sodium nitrate ($NaNO_3$, Alfa Aesar), and sodium hydroxide (NaOH, Alfa Aesar) were used as received. Technical grade sodium aluminate ($Al_2O_3{\cdot}Na_2O$, Alfa Aesar) was also used in the synthesis. The following solutions were first

* Corresponding author. Fax: +1 5307529307.
E-mail address: anavrotsky@ucdavis.edu (A. Navrotsky).

0016-7037/$ - see front matter © 2007 Elsevier Ltd. All rights reserved.
doi:10.1016/j.gca.2007.01.011

prepared: 6 M $NaNO_3$ (10.19 g in 20 ml H_2O), 2.7 M NaOH (2.18 g in 20 ml H_2O), 2 M $Na_2SiO_3{\cdot}9H_2O$ (11.44 g in 20 ml H_2O), 1 M $Al_2O_3{\cdot}Na_2O$ (3.28 g in 20 ml H_2O). Then 5 ml of each solution was mixed together in a polypropylene bottle (Nalgene) to form roughly a 20 ml gel. For oven synthesis, the plastic bottles containing the mixed solutions were heated at 90 °C for different periods of time. To check concentration effects, dilution was performed by adding 10 or 20 ml of additional water. The precipitation behavior of the gel at room temperature was also investigated by storing the gels in sealed bottles for pre-determined times.

For *in situ* synthesis calorimetry, the gel mixture with 10 ml additional water was investigated with a Setaram C-80 calorimeter. The procedure was similar to that used in earlier studies of zeolite synthesis (Yang and Navrotsky, 2000, 2002, 2004a,b). The sample vessel holding a Teflon liner was loaded with 7.5 g of the gel and sealed. The reference vessel contained 7.5 g of water. Scanning mode was used to study the crystallization of gel with different heating rates (0.1, 0.05 and 0.01 °C/min). For runs with slower heating rates (0.05 and 0.01 °C/min), the calorimeter temperature was raised to 65 °C at 0.1 °C/min after sample loading and programmed to heat at a specified slower rate thereafter. After reaching the preset end temperature (105 °C for 0.1 °C/min scan and 97 °C for slower scans), the calorimeter was kept at that temperature for 48 h to ensure complete reaction. Each synthesis calorimetric experiment was completed by repeating the same heating sequences again for baseline correction. A flat baseline in the second run confirmed completion of synthesis in the first run. For the synthesis experiment performed with a heating rate of 0.1 °C/min, samples were collected before, during, and after the crystallization peak for phase identification; the sample vessel was removed from the calorimeter at a preset temperature during the calorimetric experiment and immediately cooled to room temperature with running cold water. To assist the interpretation of *in situ* synthesis, conversion experiments from zeolite A to sodalite were also performed, in which 1 g zeolite A (NIST reference material), 6 g $NaNO_3$ and 2 g NaOH were mixed with 40 ml H_2O and heated at various temperatures in sealed plastic bottles in an oven. All samples were centrifuged and washed repeatedly with distilled water to neutral pH and dried at 40 °C before analysis.

Phase identification was performed on an Inel XRG 3000 X-ray diffractometer (Ni-filtered Cu Kα radiation, 30 kV and 30 mA). The position-sensitive detector has a resolution of 0.029° 2θ. Selected samples were also characterized by high resolution scanning electron microscopy (Philips FEI XL30).

The conditions and products of all syntheses are summarized in Table 1.

3. RESULTS

3.1. Oven synthesis

The gel-like mixtures produced by mixing sodium silicate, sodium nitrate, sodium hydroxide and sodium aluminate solutions had been placed in a lab oven pre-heated at 90 °C for up to five days. X-ray diffraction patterns of the end products are shown in Fig. 1. The unnamed zeolite

Table 1
Summary of syntheses
(A) In situ, oven, and room temperature syntheses[a]

Experiment	Water addition (ml)	Heating history	Products
In situ synthesis	10	From R.T.[b] to 105 °C at 0.1 °C/min or 97 °C at slower heating rates followed by isothermal heating at this temperature for 48 hours. Above sequences were repeated for baseline correction after the calorimeter was cooled down to R.T.	Sodalite, Cancrinite (minor)
Aging time effect (oven)	0	Aging at 90 °C for up to 5 days	Sodalite, Cancrinite (minor)
Dilution effect (oven)	10	Aging at 90 °C for 2 days	Zeolite A (minor), Sodalite
	20		Zeolite A, Sodalite (minor)
R.T. synthesis	10	R.T. for up to 3 weeks	Zeolite A

(B) Zeolite A to sodalite conversion

Experiment	Synthesis conditions				Heating history	Products
	Zeolite A (g)	$NaNO_3$ (g)	NaOH (g)	H_2O (ml)		
In situ synthesis	1	6	2	40	From R.T. to 105 °C at 0.1 °C/min followed by isothermal heating at this temperature for 48 hours. Above sequences were repeated for baseline correction after the calorimeter was cooled down to R.T.	Sodalite, Cancrinite (minor)
Oven synthesis	1	6	2	40	Aging at 60 and 70 °C for 24 h	Zeolite A, Sodalite (minor)
					Aging at 80 and 90 °C for 24 h	Sodalie, Cancrinite (minor)

[a] The starting material for all synthesis is the reaction product by mixing 5 ml of each of the following solutions: 6 M $NaNO_3$, 2.7 M NaOH, 2 M $Na_2SiO_3{\cdot}9\ H_2O$, 1 M $Al_2O_3{\cdot}Na_2O$. Water is added during the mixing.

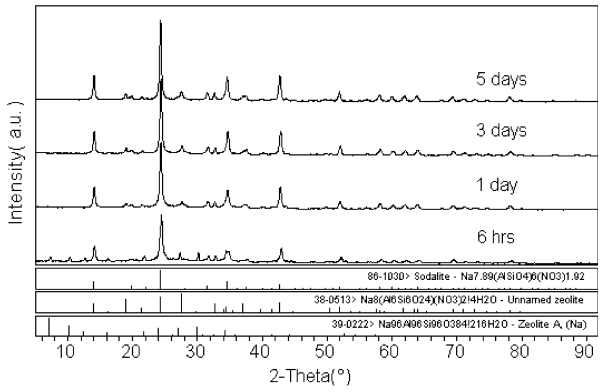

Fig. 1. X-ray diffraction pattern showing precipitation behavior of mixed solution of sodium silicate, sodium nitrate, sodium hydroxide and sodium aluminate at 90 °C.

(PDF#38-0513) refers to nitrate cancrinite in the PDF database. After only 6 hours of aging, the precipitate consists of nitrate sodalite (PDF#86-1030) as the dominant phase and a small amount of zeolite A (PDF#39-0222). Zeolite A can no longer be seen after 1 day of aging, indicating that the transformation from zeolite A to sodalite is relatively fast. A minor amount of nitrate cancrinite (PDF#38-0513) impurity appears at 1 day of aging and is seen throughout the rest of the synthesis. Thus zeolite A is the first phase formed in the mixed solution and its disappearance is associated with the formation of sodalite in a relatively rapid process. With increasing aging time, sodalite is converted into cancrinite at a very slow rate.

The concentration effect on the precipitation behavior of the gel-like mixture was also investigated by diluting it with 10 and 20 ml water. In this case, all samples were heated in an oven at 90 °C for 48 h. Comparison of the XRD patterns of the end products (Fig. 2) shows that the amount of zeolite A increases with dilution. Although the amount of zeolite A is minor with 10 ml water addition, the product consists of mostly zeolite A when the gel is diluted with 20 ml water, suggesting lower solution concentrations favor

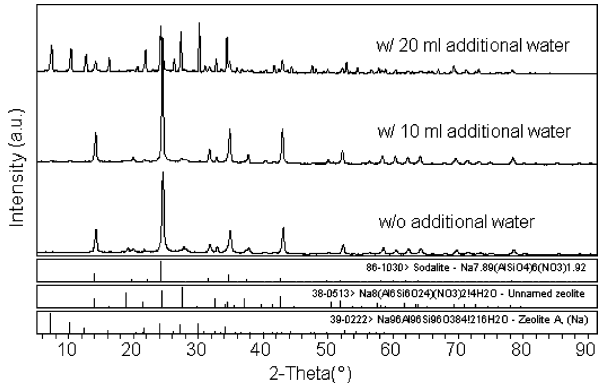

Fig. 2. X-ray diffraction pattern showing dilution effect on the precipitation behavior of mixed solution of sodium silicate, sodium nitrate, sodium hydroxide and sodium aluminate at 90 °C with 48 h aging.

the formation of zeolite A. The recipe with 10 ml water dilution was used in *in situ* calorimetry experiments because of easier loading of the gel-like mixture into the reaction vessel.

3.2. Precipitation at room temperature

After the addition of 10 ml water to the gel obtained by mixing sodium silicate, sodium nitrate, sodium hydroxide and sodium aluminate solutions, the mixture was kept at room temperature. XRD analysis showed that zeolite A precipitated within 2 weeks and complete crystallization of zeolite A occurred after 3 weeks of aging (Fig. 3). Precipitation of zeolite A from the mixed solution at room temperature suggests that zeolite A is an intermediate, possibly metastable phase that forms before sodalite crystallization.

3.3. Zeolite A to sodalite conversion

To investigate further the phase transformation behavior, zeolite A was loaded in a mixed solution of sodium nitrate and sodium hydroxide. The mixture was aged at different temperatures in an oven for 24 h. Similar to the findings in the oven synthesis, the product was sodalite with a small amount of cancrinite at temperatures of 80 and 90 °C (Fig. 4). No significant amounts of sodalite were formed from zeolite A in the solution at temperatures lower than 70 °C. Therefore, rapid conversion of zeolite A to sodalite under current conditions only takes place at temperatures higher than 70 °C.

The rate of phase transformation from zeolite A to sodalite/cancrinite at 90 °C was also investigated. Data indicated that the reaction was completed within 8 h of aging. No conversion was found at room temperature even after 46 days storage of the reaction mixture.

3.4. *In situ* synthesis calorimetry

During the initial heating and subsequent isothermal segments, heat flow peaks were only found in the scanning mode. No peaks were detected in the second run when repeating the same heating sequences for baseline correc-

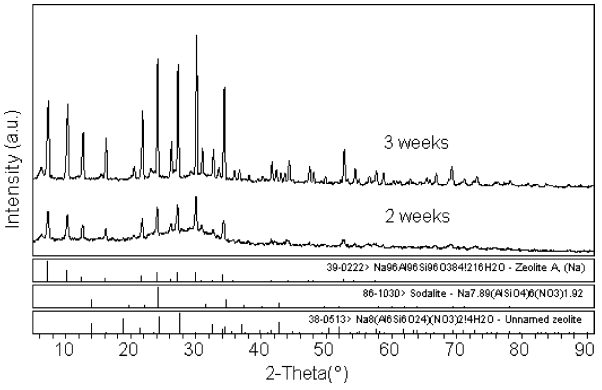

Fig. 3. X-ray diffraction pattern showing precipitation behavior of the gel-like mixture at room temperature.

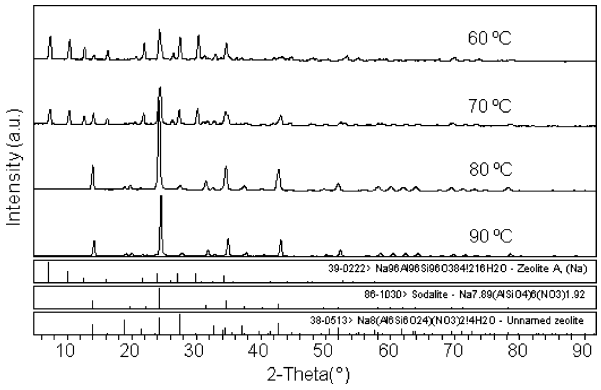

Fig. 4. X-ray diffraction pattern showing zeolite A to sodalite conversion at different temperatures with 24 h aging.

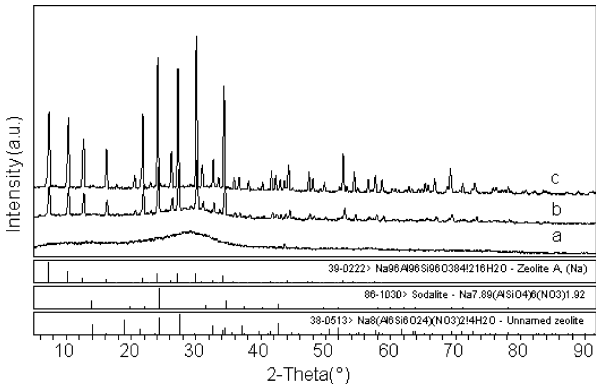

Fig. 6. X-ray pattern for *in situ* synthesis calorimetry at a heating rate of 0.1 °C/min. Sampling temperature was: (a) 68.36 °C; (b) 82.50 °C; and (c) 92.40 °C.

tion. The heat effects (corrected for baseline) related to the crystallization of the solution mixture at three heating rates are shown in Fig. 5. All three syntheses show one strong exothermic peak typical of crystallization. Crystallization occurs at lower temperature with slower heating rate. The enthalpies of crystallization for the syntheses with 0.1, 0.05 and 0.01 °C/min heating rate are −0.36, −0.34 and −0.33 J per gram of gel. Although the peak height decreases with slower heating rate, the magnitude of the integrated exothermic heat effect is almost unchanged. This indicates that heating rate has little influence on the completeness of crystallization. Crystallization takes a longer time with slower heating, but all samples finish precipitation within hours.

Samples were also collected before, during, and after the crystallization exotherm for phase identification. For the sample with a heating rate of 0.1 °C/min, sampling temperatures were chosen as 68.4, 82.5 and 92.4 °C. Fig. 6 shows the X-ray patterns of the collected samples. The sample collected at 68.4 °C before the appearance of the crystallization peak was amorphous. Significant amount of crystallization took place in the sample collected at 82.5 °C. The sample was completely crystallized at the end of the peak (92.4 °C). The crystalline phase was identified as zeolite A.

However, the end product after the entire *in situ* experiment was found to be mostly sodalite with a minor amount of cancrinite (Fig. 7), similar to the precipitation behavior observed for oven synthesis. Fig. 8 shows the SEM image of a typical sodalite product from in situ calorimetric synthesis. Heat flow peaks related to the conversion of zeolite A to sodalite/cancrinite were not seen in either heating or isothermal segments of the calorimetric runs. Similarly, when a mixture of zeolite A, $NaNO_3$ and NaOH was loaded in the calorimeter, no heat flow peaks were detected during the entire scan, although zeolite A was transformed to sodalite in the end according to XRD analysis.

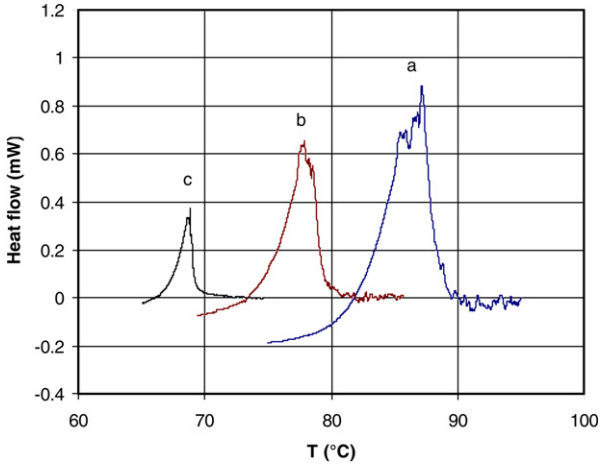

Fig. 5. *In situ* calorimetry of gel mixture at different heating rates. The heating rates of the three scans were: (a) 0.1 °C/min; (b) 0.05 °C/min; (c) 0.01 °C/min.

4. DISCUSSION

Our synthesis experiments demonstrate that precipitation of nitrate sodalite from mixed solutions of sodium silicate, sodium nitrate, sodium hydroxide and sodium aluminate is a relatively rapid process. It takes less than a day at 90 °C for sodalite to precipitate. Slower heating promotes the precipitation of zeolite A at lower temperatures and slows the formation of sodalite (Fig. 5). The transformations follow a pathway of amorphous–zeolite A–sodalite–cancrinite, which is consistent with the literature (Barnes et al., 1999a; Mattigod et al., 2002). Zeolite A is believed to nucleate and crystallize from a solution coexisting with the amorphous phase and this solution is supersaturated with respect to the zeolite A (Hu and Lee, 1990). The solution coexisting with zeolite A, with equilibrium established before the onset of sodalite nucleation, is then supersaturated with respect to sodalite (Subotic et al., 1980; Subotic and Sekovanic, 1986). The final transformation from sodalite to cancrinite is the slowest solution-mediated process (Barnes et al., 1999a).

Our data also indicate that lower temperatures and solution concentrations favor the formation of zeolite A (Figs. 2–4). Zeolite A can even precipitate at room temperature given long enough crystallization time (up to 3 weeks under current solution concentration). At higher temperatures

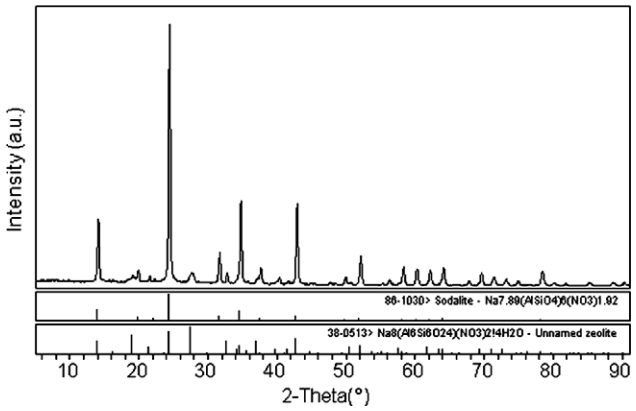

Fig. 7. X-ray pattern for the final product of an *in situ* calorimetry experiment. The sample was heated to 105 °C at 0.1 °C/min followed by a 48 h isothermal treatment. The entire heating sequences were repeated for baseline correction afterwards.

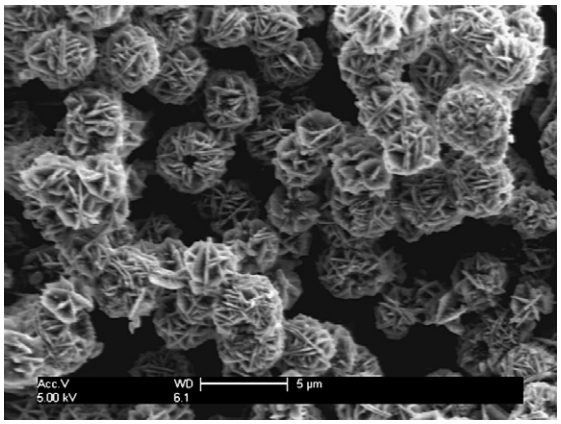

Fig. 8. SEM image of sodalite obtained after *in situ* synthesis at a heating rate of 0.1 °C/min.

and concentrations, zeolite A transforms to sodalite at accelerated rates. Breuer et al. (1963) reported similar temperature- and concentration-sensitive transformation of zeolite A to sodalite. These phase transformation phenomena are most likely kinetically controlled. It is known that the solubility of both zeolite A and sodalite increases with temperature and zeolite A has higher solubility than sodalite (Breuer et al., 1963). The rate of zeolite A dissolution is probably faster at higher temperature. Thus the solution supersaturation level is higher and the sodalite nucleation is enhanced, resulting in faster transformation of zeolite A to sodalite with increasing temperature. Higher solution concentration has a similar effect in enhancing sodalite nucleation. The competition of kinetic factors favoring metastable phases and thermodynamic factors favoring stable ones can result in simultaneous nucleation of zeolite A and sodalite and/or sodalite and cancrinite at higher concentration and temperature ranges. The kinetically controlled reaction sequence is further supported by comparison of activation energies for zeolite A-to-sodalite and sodalite-to-cancrinite transformations, which are 104 and 133 kJ/mol, respectively (Barnes et al., 1999a,b). The activation energy for zeolite A-to-sodalite conversion is somewhat lower, suggesting a faster phase transformation rate.

In situ calorimetric study is consistent with the findings of oven synthesis for transformation behavior of the gel-like mixture. It is more revealing in that only heat flow peaks related to zeolite A formation are observed, even though the end product consists of mainly sodalite. There are two possibilities for this observation. First, if the transition from zeolite A to sodalite is a very slow process, the heat flow signal will be too spread out with time during heating and will likely be buried in the noise. However, oven synthesis experiments showed that, although slower than the precipitation of zeolite A from the mixed solution, zeolite A to sodalite transformation is still a fast process requiring no longer than 6 h at 90 °C. Heat flow signals related to such crystallization times are well within the detection capability of the C-80 calorimeter, as shown in this study for zeolite A formation at three different heating rates (Fig. 5).

On the other hand, zeolite A and nitrate sodalite may have similar enthalpies of formation and thus the enthalpy change associated with the transformation may be below the detection limit of the calorimeter. Zeolite A is structurally related to sodalite and consists of a double unit cell of sodalite without additional salt inclusion (NaCl, NaOH or $NaNO_3$) (Barrer et al., 1959). The standard enthalpy of formation from oxides of hydrated zeolite A (NIST Standard Reference Material 8851, $(Na_2O)_{0.2530}(Al_2O_3)_{0.2508}(SiO_2)_{0.4984}{\cdot}1.092H_2O$) is -74.2 ± 0.7 kJ/mol on TO_2 (T = Al or Si) basis (Cavanagh and Watters, 2006). The standard enthalpy of formation of ideal sodalite ($Na_8(Al_6Si_6O_{24})Cl_2$) was reported previously (Komada et al., 1995). Using thermodynamic cycles shown in Table 2, the enthalpy of formation from oxides and sodium chloride of the ideal sodalite was determined as -75.0 ± 1.2 kJ/mol-TO_2. The enthalpy of formation of hydroxysodalite (ideally $Na_8(Al_6Si_6O_{24})(OH)_2$) from quartz, corundum, sodium oxide, water and sodium hydroxide is -79.6 ± 1.2 kJ/mol-TO_2 (Moloy et al., 2006). In addition, pure nitrate cancrinite has an enthalpy of formation (from oxides, sodium nitrate and water) of -75.3 ± 1.3 kJ/mol-TO_2 (Liu et al., 2005). Comparison of these thermodynamic

Table 2
Calculation of the enthalpy of formation of ideal sodalite [$Na_8(Al_6Si_6O_{24})Cl_2$] from oxides and NaCl

3 Na_2O (s, 298 K) + 3Al_2O_3 (s, 298 K) + 6SiO_2 (s, 298 K) + 2NaCl (s, 298 K) → $Na_8(Al_6Si_6O_{24})Cl_2$ (s, 298 K)	ΔH_1
6Na (s, 298 K) + 3/2O_2 (g, 298 K) → 3Na_2O (s, 298 K)	$\Delta H_2 = 3 \times (-414.8 \pm 0.3) = -1244.4 \pm 0.9$ kJ[a]
6Al (s, 298 K) + 9/2O_2 (g, 298 K) → 3Al_2O_3 (s, 298 K)	$\Delta H_3 = 3 \times (-1675.7 \pm 1.3) = -5027.1 \pm 3.9$ kJ[a]
6Si (s, 298 K) + 6O_2 (g, 298 K) → 6SiO2 (s, 298 K)	$\Delta H_4 = 6 \times (-910.7 \pm 1.0) = -5464.2 \pm 6.0$ kJ[a]
2Na (s, 298 K) + Cl_2 (g, 298 K) → 2NaCl (s, 298 K)	$\Delta H_5 = 2 \times (-411.3 \pm 0.1) = -822.6 \pm 0.2$ kJ[a]
8Na (s, 298 K) + 6 Al (s, 298 K) + 6Si (s, 298 K) + 12O_2 (g, 298 K) + Cl_2 (g, 298 K) → $Na_8(Al_6Si_6O_{24})Cl_2$ (s, 298 K)	$\Delta H_6 = -13458.2 \pm 16.0$ kJ/mol[b]
$\Delta H_1 = \Delta H_6 - (\Delta H_2 + \Delta H_3 + \Delta H_4 + \Delta H_5) = -899.9 \pm 14.3$ kJ/mol $= -75.0 \pm 1.2$ kJ/mol-TO_2[c]	

[a] Robie and Hemingway (1995).
[b] Komada et al. (1995).
[c] On TO_2 (T = Al or Si) basis, the enthalpy of formation of ideal sodalite was calculated as -75.0 ± 1.2 kJ/mol.

data suggests that the differences in the enthalpies of formation among zeolite A, sodalite and cancrinite (of comparable composition) are small. Therefore, the energies associated with zeolite A-to-sodalite and sodalite-to-cancrinite conversions should be small quantities, which are difficult to differentiate by calorimetry. The standard enthalpy of formation of pure nitrate sodalite has yet to be measured.

In situ synthesis calorimetry is capable of measuring the heat effects related to nucleation and crystallization and phase transformations. Nucleation and crystallization of zeolite A from the solution release a large amount of energy, which is represented by its crystallization energy. This event is easily detected by the *in situ* calorimeter and displayed as the crystallization peaks shown in Fig. 5. In contrast, the energy of the phase transformations is much smaller and thus difficult to identify.

These findings have direct relevance to radioactive waste management in that the environment in the alkaline waste tanks can be quite similar to our experimental conditions in terms of solution composition (Ondrejcin, 1974; Agnew and Watkin, 1994). The heat released from radioactive decay causes tank waste to boil and the temperature may remain above ambient for many years (Wan et al., 2002). Volume-reduction operations not only heat waste to ~100 °C, but also change the solution concentrations. Thus, depending on the treatment history of the nuclear waste, zeolite A, sodalite and/or cancrinite may precipitate separately or together. The precipitation of aluminosilicates is a rapid process on the order of days or less. Although the enthalpies of formation of zeolite A and sodalite from oxides might be very similar, the transformation from zeolite A to sodalite is fast and spontaneous at elevated temperatures. Therefore, the more stable sodalite and cancrinite phases will likely dominate the aluminosilicate precipitates in the nuclear waste.

5. CONCLUSIONS

Both oven and *in situ* calorimetric syntheses confirmed the precipitation sequence of silicates in the order of amorphous–zeoliteA–sodalite–cancrinite. Although these depend on reaction temperature and solution concentration, the first two transformations take place rather rapidly within hours to days. The sodalite to cancrinite conversion is the slowest process. While all evidence supports the fact that zeolite A is readily transformed to sodalite, this reaction cannot be detected by *in situ* calorimetry, suggesting the enthalpies of formation of these two materials are very similar. The transformations among sodium aluminosilicate precipitates are kinetically controlled processes.

ACKNOWLEDGMENTS

The authors thank Dr. Carlos F. Jove-Colon and Dr. Francois R. Bonhomme for suggestions on some of the syntheses. We appreciate comments from Richard Wirth, Guy Hovis, Associate Editor Kelly Russell, and an anonymous reviewer. This work was supported by DOE Grant DE FG07 01ER63298.

REFERENCES

Agnew S. F., and Watkin J. G. (1994) *Estimation of Limiting Solubilities of Non-Radioactive Ionic Species in Hanford Waste Tank Supernates*. LAUR-94-3590, Los Alamos National Laboratory, Los Alamos, NM.

Barnes M. C., Addai-Mensah J., and Gerson A. R. (1999a) The mechanism of the sodalite-to-cancrinite phase transformation in synthetic spent Bayer liquor. *Micropor. Mesopor. Mater.* **31**, 287–302.

Barnes M. C., Addai-Mensah J., and Gerson A. R. (1999b) A methodology for quantifying sodalite and cancrinite phase mixtures and the kinetics of the sodalite to cancrinite phase transformation. *Micropor. Mesopor. Mater.* **31**, 303–319.

Barrer R. M., Baynham J. W., Bultitude F. W., and Meier W. M. (1959) Hydrothermal chemistry of the silicates. Part VIII. Low-temperature crystal growth of aluminosilicates, and of some gallium and germanium analogues. *J. Chem. Soc.*, 195–206.

Bickmore B. R., Nagy K. L., Young J. S., and Drexler J. W. (2001) Nitrate-cancrinite precipitation on quartz sand in simulated Hanford tank solutions. *Environ. Sci. Technol.* **35**, 4481–4486.

Breuer R. G., Barsotti L. R., and Kelly A. C. (1963) Behavior of silica in sodium aluminate solutions. *International Symposium on the Extract Metallurgy of Aluminium*, Interscience, New York, pp. 133–157.

Cavanagh R. R., and Watters, Jr., R. L. (2006) Report of investigation; RM 8851-Linde type A zeolite. *Nat. Inst. Stand. Technol.*

Hu H. C., and Lee T. Y. (1990) Synthesis kinetics of zeolite A. *Ind. Eng. Chem. Res.* **29**, 749–754.

Komada N., Westrum, Jr., E. F., Hemingway B. S., Zolotov M.-Yu., Semenov Y. V., Khodakovsky I. L., and Anovitz L. M. (1995) Thermodynamic properties of sodalite at temperatures from 15 K to 1000 K. *J. Chem. Thermodynamics* **27**, 1119–1132.

Liu Q., Xu H., and Navrotsky A. (2005) Nitrate cancrinite: Synthesis, characterization, and determination of the enthalpy of formation. *Micropor. Mesopor. Mater.* **87**, 146–152.

Liu Q., Navrotsky A., Jove-Colon C. F., and Bonhomme F. (2007) Energetics of cancrinite: effect of salt inclusion. *Micropor. Mesopor. Mater.* **98**, 227–233.

Mattigod S. V., Parker K. E., Hobbs D. T., and McCready D. E. (2002) *Precipitation of Aluminum Containing Species in Tank Wastes*. Report PNNL-13881. Pacific Northwest National Laboratories (PNNL), Richland, WA.

Moloy E. C., Liu Q., and Navrotsky A. (2006) Formation and hydration enthalpies of the hydrosodalite family of materials. *Micropor. Mesopor. Mater.* **88**, 283–292.

Ondrejcin R. S. (1974) *Chemical compositions of supernates stored in SRP high level waste tanks. DP-1347*. Savannah River Laboratory, Aiken, SC.

Qafoku N. P., Ainsworth C. C., Szecsody J. E., Bish D. L., Young J. S., McCready D. E., and Qafoku O. S. (2003) Aluminum effect on dissolution and precipitation under hyperalkaline conditions: II. Solid phase transformations. *J. Environ. Qual.* **32**, 2364–2372.

Qafoku N. P., Ainsworth C. C., Szecsody J. E., and Qafoku O. S. (2004) Transport-controlled kinetics of dissolution and precipitation in the sediments under alkaline and saline conditions. *Geochim. Cosmochim. Acta* **68**, 2981–2995.

Robie R. A., and Hemingway B. S. (1995) Thermodynamic Properties of minerals and related substances at 298.15 K and 1 bar (10^5 Pascals) pressure and at higher temperatures, Geological Survey Bulletin No. 2131.

Subotic B., and Sekovanic L. (1986) Transformation of zeolite A into hydroxysodalite: II. Growth kinetics of hydroxysodalite microcrystals. *J. Cryst. Growth* **75**, 561–572.

Subotic B., Masic N., Smit I., and Sekovanic L. (1980) Transformation of zeolite A into hydroxysodalite: I. An approach to the mechanism of transformation and its experimental evaluation. *J. Cryst. Growth* **50**, 498–508.

Su Y., Li L., Yound J. S., and Balmer M. L. (2000) Chemical and thermal stability studies of Cs-loaded IE-911. *EMSL Interfacial Chemistry and Engineering 2000 Annual Report*. Environmental Molecular Sciences Laboratory, Richland WA, pp. 7–10 to 7–11.

Wan J., Tokunaga T. K., Saiz E., Olson K. R., and Larsen J. T. (2002) Colloid formation resulting from highly alkaline and saline waste tank solution leaking into sediments at the Hanford site. Report LBID-2446. Earth Sciences Division, Lawrence Berkeley National Laboratory.

Yang S., and Navrotsky A. (2000) In situ calorimetric, structural, and compositional study of zeolite synthesis in the system $5.15Na_2O$–$1.00Al_2O_3$–$3.28SiO_2$–$165H_2O$. *J. Phys. Chem. B* **104**, 6071–6080.

Yang S., and Navrotsky A. (2002) An in situ calorimetric study of zeolite crystallization kinetics. *Micropor. Mesopor. Mater.* **52**, 93–103.

Yang S., and Navrotsky A. (2004a) Early-stage reactions in synthesis of TPA-silicate-1: studies by in situ calorimetry, SAXS, and pH measurements. *Chem. Mater.* **16**, 3682–3687.

Yang S., and Navrotsky A. (2004b) In situ calorimetric study of the growth of silica TPA-MFI crystals from an initially clear solution. *Chem. Mater.* **14**, 2803–2811.

Associate editor: J. Kelly Russell